Mississippi State University

Center for Air Sea Technology

A SEMI-IMPLICIT FREE SURFACE FORMULATION FOR THE SEMI-COLLOCATED GRID DIECAST OCEAN MODEL

by
David E. Dietrich and Avichal Mehra

Technical Report 03-98

15 APRIL 1998

Prepared for: Office of Naval Research
Under Grants N00014-97-1-0525
and N00014-97-1-0099

TECHNICAL REPORT 03-98

A SEMI-IMPLICIT FREE SURFACE FORMULATION FOR THE SEMI-COLLOCATED GRID DIECAST OCEAN MODEL

by

DAVID E. DEITRICH[1] and AVICHAL MEHRA[2]

[1] Senior Research Scientist, Mississippi State University Center for Air Sea Technology, Stennis Space Center, MS 39529-6000

[2] Postdoctoral Assistant, Mississippi State University Center for Air Sea Technology, Stennis Space Center, MS 39529-6000

15 APRIL 1998

This research was supported by the Department of the Navy, Office of Naval Research under Grants N00014-97-1-0525 and N00014-97-1-0099 with Mississippi State University. The opinion, findings, conclusions, and recommendations expressed in this publication are those of the authors and do not necessarily reflect the views of the U.S. Government. No official endorsement should be inferred.

Table of Contents

A SEMI - IMPLICIT FREE SURFACE FORMULATION FOR A SEMI-COLLOCATED GRID DIECAST OCEAN MODEL

ABSTRACT

We present a semi-implicit free-surface formulation for the DieCAST Ocean model that retains the accurate, low dissipation numerics of its latest and best semi-collocated rigid-lid version. The approach involves integrating the time-implicit (trapezoidal) shallow water equations on a staggered Arakawa "c" grid, with vertically averaged baroclinic forcing terms determined on a non-staggered Arakawa "a" grid, including a fourth-order-accurate baroclinic pressure gradient. The shallow water equation numerics are virtually equivalent to standard sigma coordinate approaches for the model barotropic mode. In application to transient wind forced lake Kelvin waves, the new free-surface version gives results very close to the corresponding strongly validated rigid-lid DieCAST version (reflecting the fact that the rigid-lid barotropic mode numerics are also a sigma-like approach), and requires less than 50 percent more computing. Thus, the numerics used by both rigid-lid and free-surface DieCAST versions combines the best of z-level and sigma coordinate numerics as well as the best of "a" and "c" grid numerics.

1.1 Introduction

In many computational fluid dynamics applications, the flows are steady or slowly changing compared to the shortest time scale resolved modes. In such case, it may be desirable to take longer time steps than explicit methods (e.g., leap frog) allow, especially when nonlinear low frequency effects (if any) of the high frequency modes are parameterized (i.e., given by ad hoc relations to the lower frequency modes). Such parameterization may also include the effects of subgrid-scale modes that are not resolved either spatially or temporaly.

Semi-implicit and fully-implicit time marching methods allow these longer time steps (e.g., Kwizak and Robert, 1971; O'Brien and Hurlburt, 1972; Dietrich, et. al, 1975; Dietrich, 1975; Dietrich and Wormeck, 1985). These methods generally "slow down" the fastest (highest frequency) modes, but, as noted above, this may be acceptable. Indeed, the fastest free surface modes have only secondary effect on the ocean general circulation. This was necessary for the success of popular ocean models that use a rigid-lid approximation or semi-implicit calculation of the high frequency surface modes. In converting the popular rigid-lid Bryan-Cox model to a corresponding model having semi- implicit free surface waves, Dukowicz, et. al (1992) showed that, after initial transients, semi-implicit free surface models ocean general circulation results are virtually identical to rigid-lid models, rather independent of the time step size up to the rigid-lid stability limit.

Semi-implicit and rigid-lid models generally require solution of an elliptic equation each time step. Thus, a good elliptic solver is needed in order for them to be useful. A major advantage of *hydrostatic* ocean models is that the hydrostatic approximation reduces the elliptic equation to two dimensions, thereby greatly reducing elliptic solver requirements (compared to non-hydrostatic three-dimensional models) and allowing use of marching "error vector propagation" (EVP) methods (Roache, 1995) that are highly efficient for low- and moderate- resolution grids.

However, for very large grids (greater than O(500) points in the "cross-march" direction) EVP storage requirements can be large and sometimes EVP cannot take full advantage of vector and massively parallel supercomputers (vectorization and parallelization is usually possible only in the cross-march direction). In such case, it may be useful to combine EVP with domain decomposition (Dietrich, 1974; Dietrich, et. al, 1975; Roache, 1995), thus leading to an iterative solution procedure. Iterative procedures work best for diagonally dominant elliptic problems. The elliptic problem associated with rigid-lid ocean models is a Poisson equation (Dietrich, et. al, 1987; Dietrich, 1992) which is less diagonally dominant than the Helmholtz equation associated with semi-implicit free surface models.

It follows that, besides being able to address free-surface modes, semi-implicit free surface ocean model formulations may be useful numerically for very large grids even when the free surface modes are of secondary interest. Thus, although low-to-moderate resolution rigid-lid models may remain attractive for general circulation simulations, high resolution grids may favor semi-implicit free surface formulations.

Previously, the DieCAST ocean model has used a rigid-lid approximation. Now that the new rigid-lid semi-collocated versions have been validated by extensive Gulf of Mexico observations (Dietrich and Lin, 1997; Dietrich, 1997) we are herein led to formulate a semi-implicit free surface version that retains the demonstrated accurate, robust, low dissipation, low dispersion numerics of the latest and best rigid-lid versions.

1.2 New Semi-Implicit Free Surface Formulation for the Semi-Collocated DieCAST Ocean Model

A major reason for the success of the DieCAST ocean model has been its robust, accurate, low dispersion and low dissipation numerics. We now formulate a semi-implicit free surface version that includes its latest and best numerics (Dietrich, 1997).

First, it is convenient to write the governing time-implicit (Crank Nicolson or trapezoidal approximation) equations in terms of the two- level time averaged fields:

$$\bar{q}^t = \frac{1}{2}(q^t + q^{t+\Delta t}) \tag{1}$$

In the following equations, all time-explicit terms are given in their analytic form. They are calculated using the standard DieCAST numerics, including filtered leapfrog time integration and fourth order advection as before. The leapfrog time level, at which all explicit terms are evaluated, is at time $t + \frac{\Delta t}{2}$.

The incompressibility (mass conservation) equation is solved only on an Arakawa "c" grid (see below). The horizontal momentum conservation equations to be solved on an Arakawa "a" grid are:

$$\bar{u}^t = u^t + \frac{\Delta t}{2}[-\vec{\nabla}\cdot(u\vec{V} - \nu\vec{\nabla}u) - g\frac{\partial \bar{h}^t}{\partial x} - \frac{\partial p}{\partial x} + fv + \tau_x] \tag{2}$$

$$\bar{v}^t = v^t + \frac{\Delta t}{2}[-\vec{\nabla}\cdot(v\vec{V} - \nu\vec{\nabla}v) - g\frac{\partial \bar{h}^t}{\partial y} - \frac{\partial p}{\partial y} - fu + \tau_y] \tag{3}$$

where the wind stress τ_x, τ_y applies to top layer only. There are also transport equations for temperature and salinity, but these are not involved in the semi-implicit algorithm described here.

The solution procedure is as follows. First, we *partially* update (without surface height or baroclinic pressure gradient terms) the semi-collocated (Arakawa "a" grid) fields $\bar{u}^t$, $\bar{v}^t$ as follows:

$$\tilde{u} = u^t + \frac{\triangle t}{2}[-\vec{\nabla} \cdot (u\vec{V} - \nu\vec{\nabla}u) + fv + \tau_x] \tag{4}$$

$$\tilde{v} = v^t + \frac{\triangle t}{2}[-\vec{\nabla} \cdot (v\vec{V} - \nu\vec{\nabla}v) - fu + \tau_y] \tag{5}$$

where $\tilde{u} = \bar{u}^t + \frac{\triangle t}{2}(g\frac{\partial \bar{h}^t}{\partial x} + \frac{\partial p}{\partial x})$ and $\tilde{v} = \bar{v}^t + \frac{\triangle t}{2}(g\frac{\partial \bar{h}^t}{\partial y} + \frac{\partial p}{\partial y})$.

Next, we interpolate (to 4th order accuracy) u and v to the "c" grid locations:

$$\tilde{u}^c = interpolated\ (\tilde{u})\ and\ \tilde{v}^c = interpolated\ (\tilde{v}) \tag{6}$$

Next, we add the baroclinic pressure gradient (standard second order accurate approximation is adequate on the "c" grid):

$$u^c = \tilde{u}^c - \frac{\triangle t}{2}\frac{\partial p}{\partial x}\ and\ v^c = \tilde{v}^c - \frac{\triangle t}{2}\frac{\partial p}{\partial y} \tag{7}$$

where $p = \int_0^z \rho g dz$ is the hydrostatic baroclinic pressure head based on the known density anomaly (deviation from horizontal average), ρ .

Equations (7) include all time-explicit terms in the implicit equations for "c" grid velocity. Adding the implicit surface height gradient terms to the right hand sides of equations (7) will provide the fully updated "c" grid two-level-time-averaged velocity. We determine the surface height implicitly as follows.

Defining,

$$U = \frac{1}{H}\int_0^H u^c\ dz\ \ and\ \ V = \frac{1}{H}\int_0^H v^c\ dz \tag{8}$$

where H is the local depth ignoring small surface wave fluctuations, the implicit "c" grid barotropic mode spatially differenced equations are:

$$\bar{u}_{i,j} = -(g\frac{\triangle t}{2})\frac{\bar{h}_{i+1,j} - \bar{h}_{i,j}}{\triangle x} + U_{i,j} \tag{9}$$

$$\bar{v}_{i,j} = -(g\frac{\triangle t}{2})\frac{\bar{h}_{i,j+1} - \bar{h}_{i,j}}{\triangle y} + V_{i,j} \tag{10}$$

$$\bar{h}_{i,j} = h^t_{i,j} - \frac{\triangle t}{2}\left(\frac{H_{i+1/2,j}\ \bar{u}_{i,j} - H_{i-1/2,j}\ \bar{u}_{i-1,j}}{\triangle x} + \frac{H_{i,j+1/2}\ \bar{v}_{i,j} - H_{i,j-1/2}\ \bar{v}_{i,j-1}}{\triangle y}\right) \tag{11}$$

where $\bar{u}$ and $\bar{v}$ are vertically and two-level time averaged "c" grid quantities, not to be confused with $\bar{u}^t$ and $\bar{v}^t$ in the three-dimensional equations (2) and (3). Equations (9)-(11) are an implicit time differenced formulation of the shallow water equations. These are fundamentally an application of sigma coordinates for the barotropic mode.

Substituting equations (9) and (10) into the right hand side of equation (11) gives us a Helmholtz equation for $\bar{h}$ with sources from U and V:

$$\frac{H_{i+1/2,j}(\bar{h}_{i+1,j} - \bar{h}_{i,j}) - H_{i-1/2,j}(\bar{h}_{i,j} - \bar{h}_{i-1,j})}{(\triangle x)^2}$$

$$+ \frac{H_{i,j+1/2}(\bar{h}_{i,j+1} - \bar{h}_{i,j}) - H_{i,j-1/2}(\bar{h}_{i,j} - \bar{h}_{i,j-1})}{(\triangle y)^2}$$

$$-\frac{4}{g(\triangle t)^2}\bar{h}_{i,j} = -\frac{4}{g(\triangle t)^2}h^t_{i,j} + \frac{2}{g\triangle t}\left(\frac{H_{i+1/2,j}\ U_{i,j} - H_{i-1/2,j}\ U_{i-1,j}}{\triangle x}\right.$$

$$\left. - \frac{H_{i,j+1/2}\ V_{i,j} - H_{i,j-1/2}\ V_{i,j-1}}{\triangle y}\right) \tag{12}$$

Equation (12) is solved for $\bar{h}$. This result may be substituted into equations (9) and (10) to get barotropic "c" grid $\bar{u}$ and $\bar{v}$, but these are not really needed in this formulation.

Next, the full 3-d "c" grid advanced time level fields are updated from:

$$h^{t+\triangle t}_{i,j} = 2\ \bar{h}_{i,j} - h^t_{i,j} \tag{13}$$

$$u^{t+\triangle t}_{i,j,k} = 2u^c_{i,j,k} - g\triangle t\frac{(\bar{h}_{i+1,j} - \bar{h}_{i,j})}{\triangle x} - u^t_{i,j,k} \tag{14}$$

$$v^{t+\triangle t}_{i,j,k} = 2v^c_{i,j,k} - g\triangle t\frac{(\bar{h}_{i,j+1} - \bar{h}_{i,j})}{\triangle y} - v^t_{i,j,k} \tag{15}$$

$$w_{i,j,k} = -\int_H^z \left(\frac{u^{t+\triangle t}_{i,j,k} - u^{t+\triangle t}_{i-1,j,k}}{\triangle x} + \frac{v^{t+\triangle t}_{i,j,k} - v^{t+\triangle t}_{i,j-1,k}}{\triangle y}\right) dz \tag{16}$$

Equations (14-16) give a non-divergent 3-d advection velocity for the next time step. The vertical velocity does not vanish at the top as it does in rigid-lid formulations. Neuman conditions may be used to get reasonable advective fluxes through the open top, because the field variables generally are nearly constant over depths much larger than h variations. A more accurate approach would include time dependent control volumes in the top layer, but the present simpler approach should be adequate except in shallow water and large amplitude wave conditions (i.e., h not small compared to top layer thickness). Large dissipation occurs under such shallow water conditions, allowing appropriate parameterization through model dissipation parameters; alternatively, a more specialized surf zone model could be coupled to the present model.

Finally, the 4th order "a" grid pressure and surface height gradients are calculated and substituted into equations (2) and (3) to finalize the 3-d "a" grid solution.

The long term averaged flow resulting from the above procedure will have extremely small barotropic mode divergence, because there is no long term trend of the ocean surface height. As noted above, the short term fluctuations (the so-called "fast modes") have little effect on the ocean general circulation. It follows that the above solution procedure will yield virtually the same ocean general circulation as the earlier rigid-lid versions of the DieCAST ocean model and thus retain its robust, accurate, low dissipation and low dispersion numerics.

1.3 Procedure Summary

A semi-implicit free-surface procedure that includes the latest and best 4th order numerics in the semi-collocated DieCAST version has been given. The procedure is as follows:

1. determine advection, diffusion and Coriolis terms, and wind stress on the "a" grid
2. interpolate the results from step 1 to the "c" grid
3. evaluate the baroclinic pressure gradient on the "c" grid using the standard second order accurate "c" grid scheme and add it to the interpolated terms from the "a" grid
4. vertically average the step 3 result
5. solve the implicit trapezoidal (Crank Nicolson) shallow water equations forced by the step 4 result (combined to form a Helmholtz equation for the free surface height that is identical to the rigid lid pressure equation in the limit of large time step)
6. update the three-dimensional "c" grid velocity by adding the free-surface height gradient calculated in step 5 to the terms calculated in step 3.

7. evaluate the full pressure gradient on the "a" grid using the updated free surface height calculated in step 5 and adding the baroclinic pressure gradient (evaluated to 4th order accuracy on the "a" grid) (this is probably better than interpolating "c" grid results back to the "a" grid)

8. finish the time step using results of steps 1 and 7.

1.4 Comments on Pressure Gradient Evaluation in Semi-implicit Mixed "a" and "c" Grid Modeling

Two possible procedures regarding the pressure gradient evaluation in semi-implicit free-surface mixed "a" and "c" grid models are:

1. the above procedure, which evaluates both the baroclinic and the barotropic pressure gradient to second-order accuracy on the natural staggered "c" grid of the barotropic mode equations, and also evaluates both to fourth-order accuracy in the collocated "a" grid equations;

2. a modified procedure, which evaluates only the barotropic (sea surface height) pressure gradient terms on the "c" grid (to second-order accuracy) in the implicit barotropic mode equations. Instead evaluating the baroclinic pressure gradient on the "c" grid, the fourth-order baroclinic "a" grid pressure gradient is interpolated to the "c" grid (again using fourth-order accurate interpolations).

While the first procedure is aesthetically pleasing, we have found that it is, disappointingly, unstable when using long implicit time steps (more than a few times the explicit limit). On the other hand, the second procedure when carefully done to full fourth-order accuracy, is more accurate than the first procedure and is found to be stable with very long time steps, not limited by explicit limit. For example, we have run 40 model days (1440 time steps) with time step size $\sim$50 times the explicit limit.

A third possible procedure is to evaluate the baroclinic pressure gradient to fourth-order accuracy on the "c" grid (together with a second-order accurate barotropic pressure gradient), and to interpolate the mixed-order full pressure gradient to the "a" grid. These choices apply to rigid-lid as well as to free-surface approaches.

The barotropic mode pressure (surface height) gradient has only second-order accuracy in all three procedures. We have not tested the third procedure, because we have found the second procedure to be robust as well as reasonably accurate, as demonstrated below in Section 1.5. It gives accurate fast mode (barotropic mode gravity wave) phase speed when the fast mode time scale is resolved, and has fourth-order accuracy on the baroclinic modes that dominate ocean general circulation. Although the second procedure appears best at this time, the first and third procedure may be useful when very accurate fast mode results are desired, especially in ultra-high resolution

coastal simulations.

Having tested the second procedure in idealized applications, we are now proceeding toward real applications and iterative elliptic solver implementation as noted above.

1.5 Free-Surface Results

We now discuss application of the new free-surface DieCAST version, and the reduced dispersion rigid-lid DieCAST "a" grid version (Dietrich, 1997) to a transient-wind-forced lake Kelvin wave problem. The rigid-lid version is further enhanced by suggestions by Dr. Brian Sanderson (University of New South Wales, Australia) and Dr. Dan Wright (Bedford Institute of Oceanography, Canada).

Specifically, the free-surface and rigid-lid versions are both applied with 625 m resolution to an idealized circular flat-bottom lake patterned after summertime Great Lakes conditions, as described by Beletsky, et. al (1997). Both versions use the same physical parameters and wind forcing, including 1 m^2/sec lateral viscosity and diffusivity.

Figure 1 shows the temperature at level 9.7 m (near the thermocline) from both free-surface and rigid-lid versions at days 6, 10, 14, 22 and 30. Although the results differ by as much as five percent during the first few days, they agree within a fraction of one percent after day ten. This is because fast free-surface modes disperse, reflect and dissipate during the first ten days, during which they affect thermocline level temperatures as they slosh around the basin.

Time averaging free-surface results over 1/2 day to reduce fast mode amplitudes, and, for consistency, applying the same time average to the rigid-lid results, shows in Figure 2 that the early results are closer during the first few days.

Although highly inertial Poincare waves are strong through day 30, the solution is dominated by the Kelvin edge wave, which propagates around the 100-km diameter lake in $\sim$8 days.

These new free-surface and rigid-lid results are similar to results from the more dispersive original "a" grid DieCAST model used by Beletsky et. al (1997). However, the Kelvin wave speed is closer to the theoretical value and the results are more strongly inertial, including intense internal wave bore development after day 20. The improvement in the results is due to accurate reduced-dispersion numerics (Dietrich, 1997). The new free-surface and rigid-lid DieCAST results are much closer to each other than to the original "a" grid DieCAST rigid-lid results, although they are quite similar

to the original.

In implicit models, increasing time step size reduces phase speeds of modes having unresolved frequencies. However, when the time step resolves the wave propagation, the new semi-implicit free-surface DieCAST version gives accurate free-surface wave phase speeds of ~31 m/sec, which is the correct linear phase speed for the 100 m deep model lake. Its fourth-order accuracy on the baroclinic terms and "c" grid accuracy on the barotropic terms guarantees good accuracy when resolution is adequate. However, a notable advantage is that the time step can be many times longer than required to resolve the highest frequency resolved free surface "fast" modes. This does not destroy the accuracy of longer wavelength (and thus lower frequency) resolved free surface modes. Such long time step has little effect on the accuracy of slow internal waves and even slower baroclinic modes, or on how they affect free surface height.

With the 162 X 162 X 12 layers resolution used, the free-surface version requires ~4.5 sec cpu per time step on an SGI Indigo 2 computer, which runs at about 12.5 megaflops. This is ~4.7 percent more computation per time step than the rigid-lid version. The rigid-lid version is stable with time step up to ~600 sec. The free-surface version is stable with a 400 sec time step, and unstable with a 600 sec time step. With a 400 sec time step, the fast surface wave Courant number is ~50, indicating up to 50 times less computing compared to explicit methods. In the comparison runs, both versions were run with a 400 sec time step.

It is noteworthy that, as resolution increases, the elliptic solver computation and storage increase relative to the rest of the model. Thus, for large grids, it may be useful to explore ways to reduce the elliptic solver overhead. As noted above, a significant motivation of introducing the free surface is to reduce elliptic solver overhead on extra large grids, because increased diagonal dominance associated with the free-surface formulation benefits potentially lower overhead iterative solvers (Roache, 1995; Dietrich, et. al, 1975). For sufficiently large grids, the elliptic solver storage overhead is substantially reduced and its computation reduction should more than compensate for the slightly smaller time step required by the DieCAST free-surface version. We expect the free surface version, combined with an iterative elliptic solver, will prove especially attractive for grids larger than O(500 X 500) horizontal resolution.

Acknowledgements

We are grateful for support from the Navy Ocean Modeling and Prediction Program at the Office of Naval Research, under Research Grants N00014-97-1-0525 and N00014-97-1-0099 with Mississippi State University.

References

Beletsky, D., O'Connor, W.P., Schwab, D.J., and Dietrich, D.E., 1997. Numerical Simulation of Internal Kelvin Waves and Coastal Upwelling Fronts, *J. Phys. Oceanogr.*, 27(7), 1197-1215.

Dietrich, D.E., 1997. Application of a Modified "a" Grid Ocean Model Having Reduced Numerical Dispersion to the Gulf of Mexico Circulation, *Dynamics of Atmospheres and Oceans*, 27, pp. 201-217.

Dietrich, D.E., C.A. Lin, A. Mestas-Nunez and D.-S. Ko, 1997. A High Resolution Numerical Study of Gulf of Mexico Fronts and Eddies, *Meteorol. Atmos. Physics*, 64, pp. 187-201.

Dietrich, D.E., 1992. The Sandia Ocean Modeling System Programmers Guide and Users Manual, *Sandia National Laboratories Technical Report* SAND92-7286.

Dietrich, D.E., M.G. Marietta, and P.J. Roache, 1987. An Ocean Modeling System with Turbulent Boundary Layers and Topography, Part 1: Numerical Description, *Int. J. Numer. Methods Fluids*, 7, 833-855.

Dietrich, D.E. and J.J. Wormeck, 1985. An Optimized Implicit Scheme for Compressible Reactive Gas Flow, *Numerical Heat Transfer*, 8, 335-348.

Dietrich, D.E., 1981. A Program of Elliptic Solver Development and Implementation in Semi-Implicit Numerical Ocean Circulation Models. *JAYCOR Final Report #* J510-81-053/2192 (Sponsored by the Office of Naval Research and Naval Ocean Research and Development Activity).

Dietrich, D.E., 1975. Numerical Solution of Fully-Implicit Energy Conserving Primitive Equations, *J. Meteor. Soc. Japan*, 53, 222-225.

Dietrich, D.E., B.E. McDonald, and A. Warn-Varnas, 1975. Optimized Block- Implicit Relaxation, *J. Comp. Phys.*, 18, 421-439.

Dietrich, D.E., 1974. Comments on A Direct Solution of Poisson's Equation by Generalized Sweep-Out Method, *J. Meteor. Soc. Japan*, 52, 337-338.

Dukowicz, J.K., R.D. Smith and R.C. Malone, 1992. A Reformulation and Implementation of the Bryan-Cox-Semtner Ocean Model on the Connection Machine, *Los Alamos National Laboratory Report* LA-UR-91-2864.

Kwizak, M. and A. Robert, 1971. A Semi-Implicit Scheme for Grid Point Atmospheric Models of the Primitive Equations. *Mon. Wea. Rev.*, 94, 32-36.

O'Brien, J.J. and H.E. Hurlburt, 1972. A Numerical Model of Coastal Upwelling. *J. Phys. Oceanogr.*, 2, 14-26.

Roache, P.J., 1995. *Elliptic Marching Methods and Domain Decomposition.* CRC Press, 190 pp.

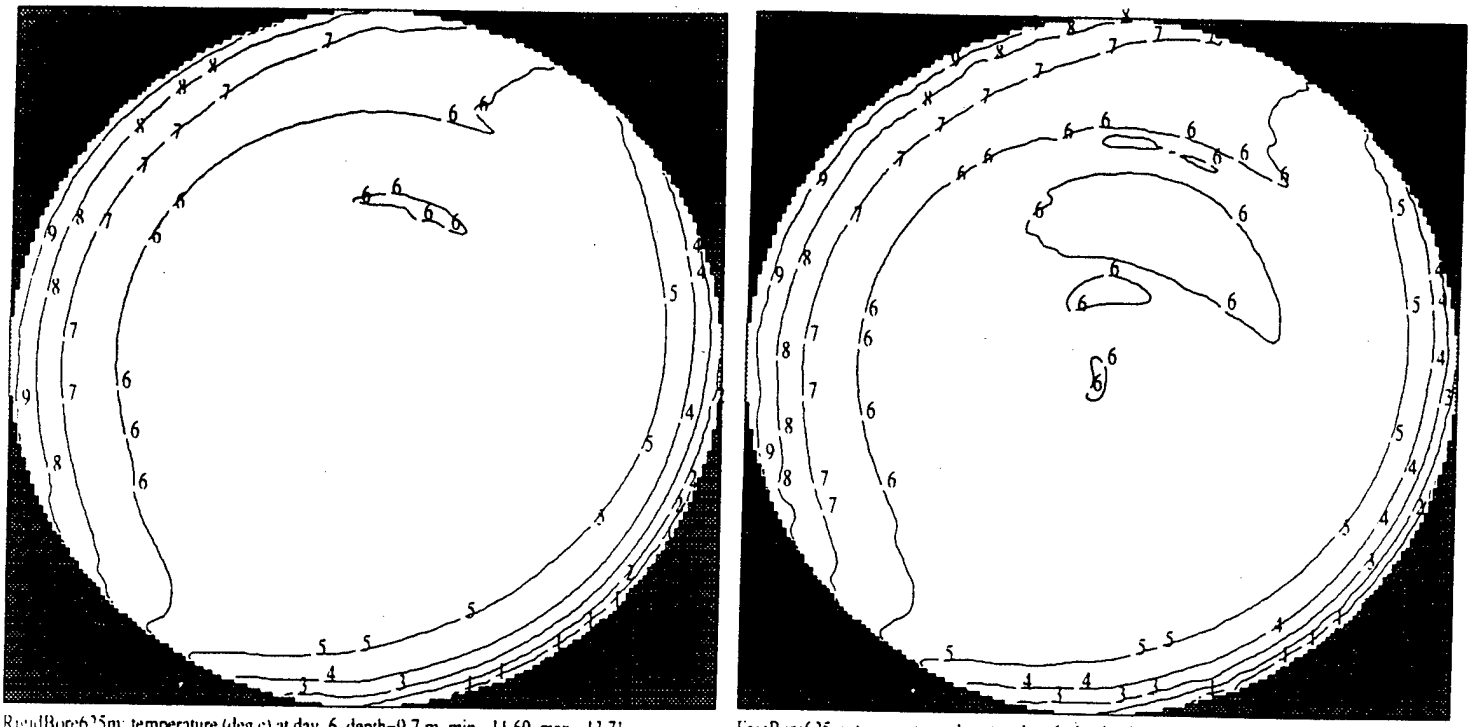

Figure 1: Comparison of temperature at level 9.7 m (near the thermocline) from rigid-lid (left) and free-surface (right) versions at days 6, 10, 14, 22 and 30.

RigidBore625m: temperature (deg c) at day 10, depth=9.7 m. min= 11.83, max= 13.69

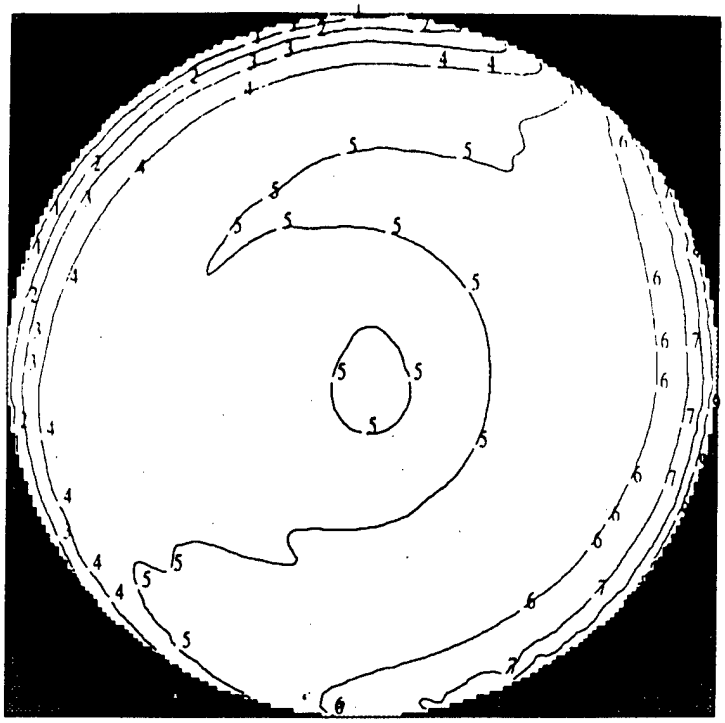

FreeBore625m: temperature (deg c) at day 10, depth= 9.7 m. min= 11.83, max= 13.65

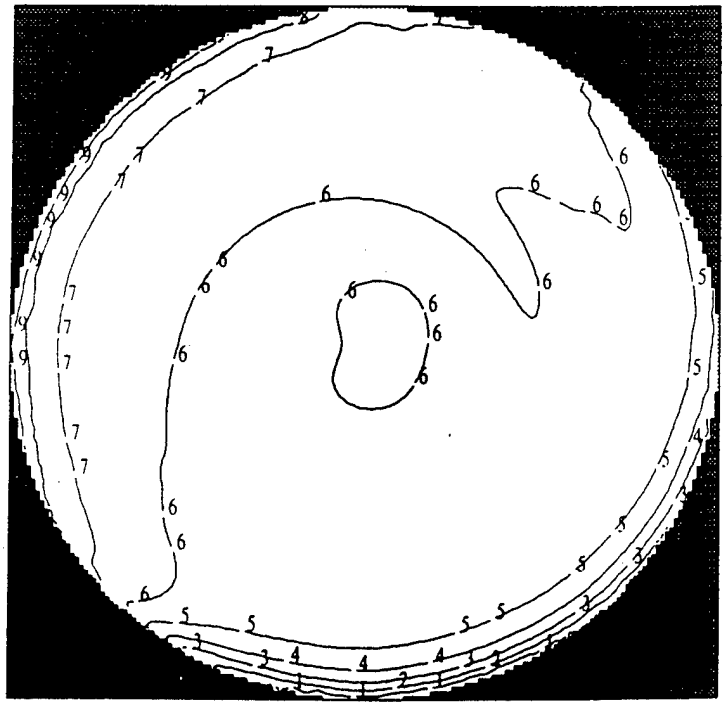

RigidBore625m: temperature (deg c) at day 14, depth=9.7 m. min= 11.70, max= 13.36

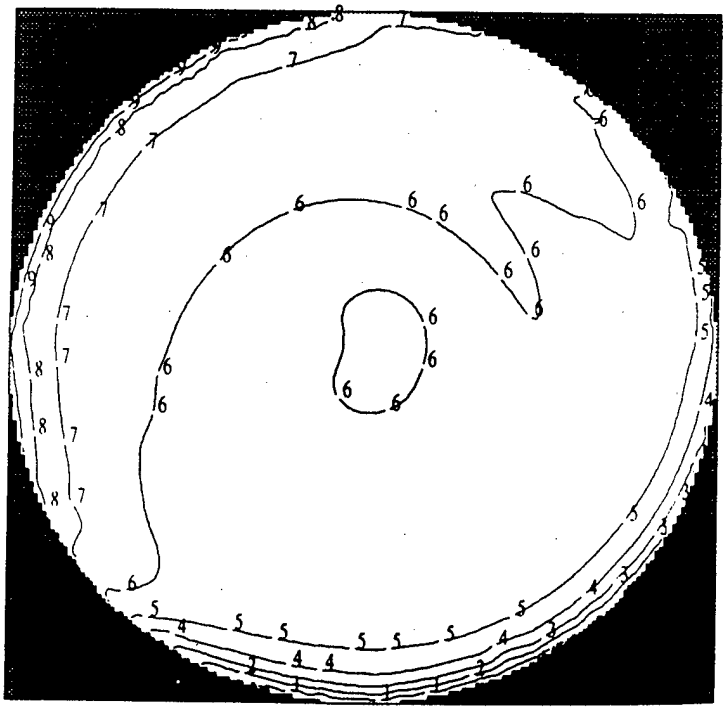

FreeBore625m: temperature (deg c) at day 14, depth= 9.7 m. min= 11.70, max= 13.37

Figure 1: (Cont.)

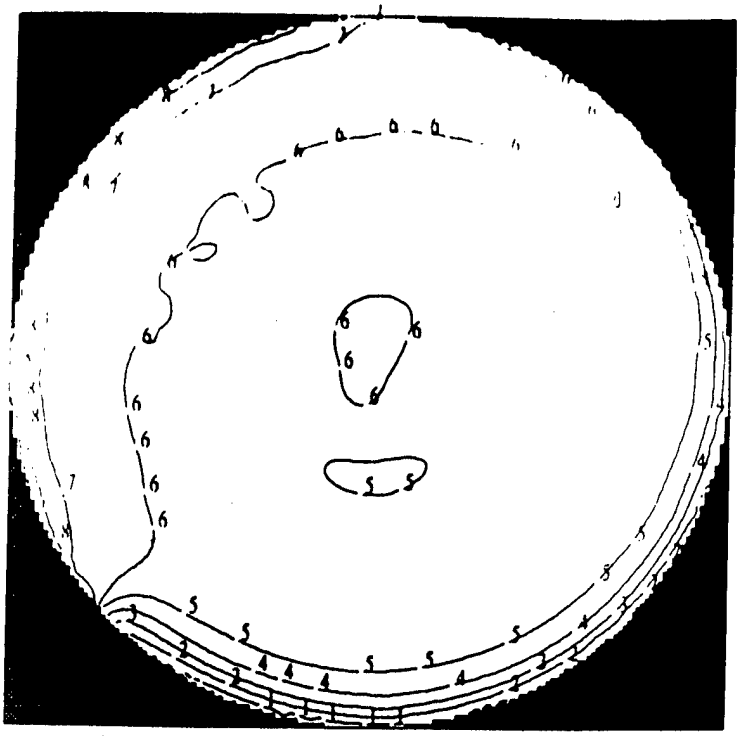

RigidBore625m: temperature (deg c) at day 22, depth=9.7 m. min= 11.93, max= 13.08

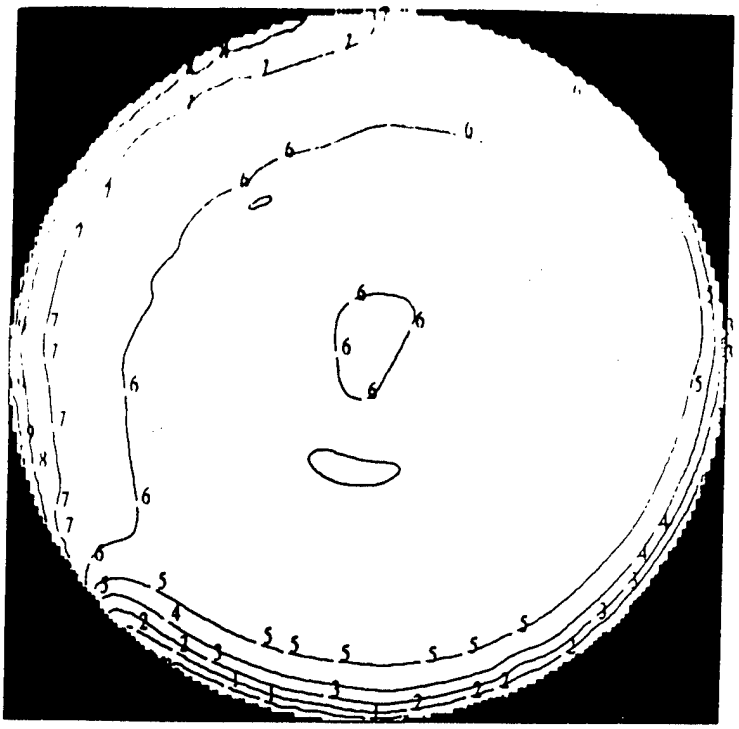

FreeBore625m: temperature (deg c) at day 22, depth= 9.7 m. min= 11.94, max= 13.08

RigidBore625m: temperature (deg c) at day 30, depth=9.7 m. min= 12.10, max= 12.79

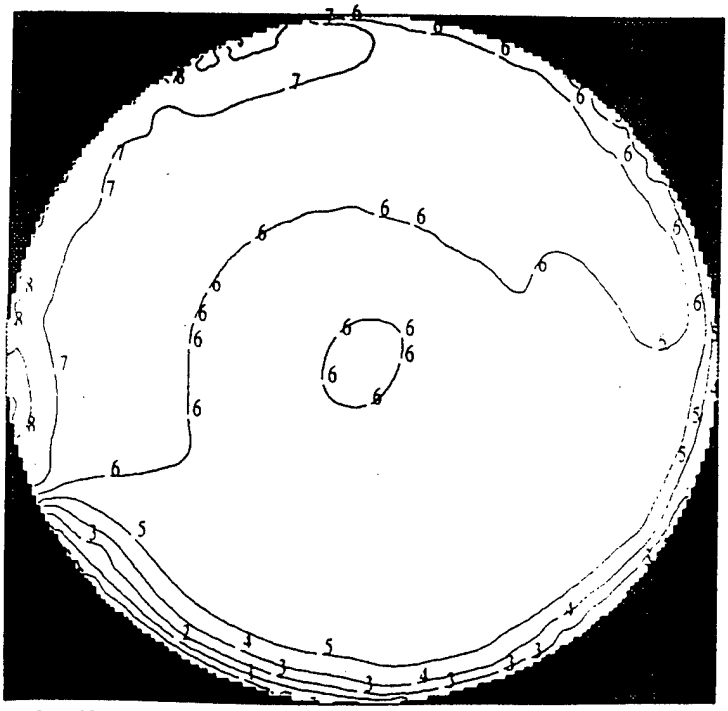

FreeBore625m: temperature (deg c) at day 30, depth= 9.7 m. min= 12.10, max= 12.78

Figure 1: (Cont.)

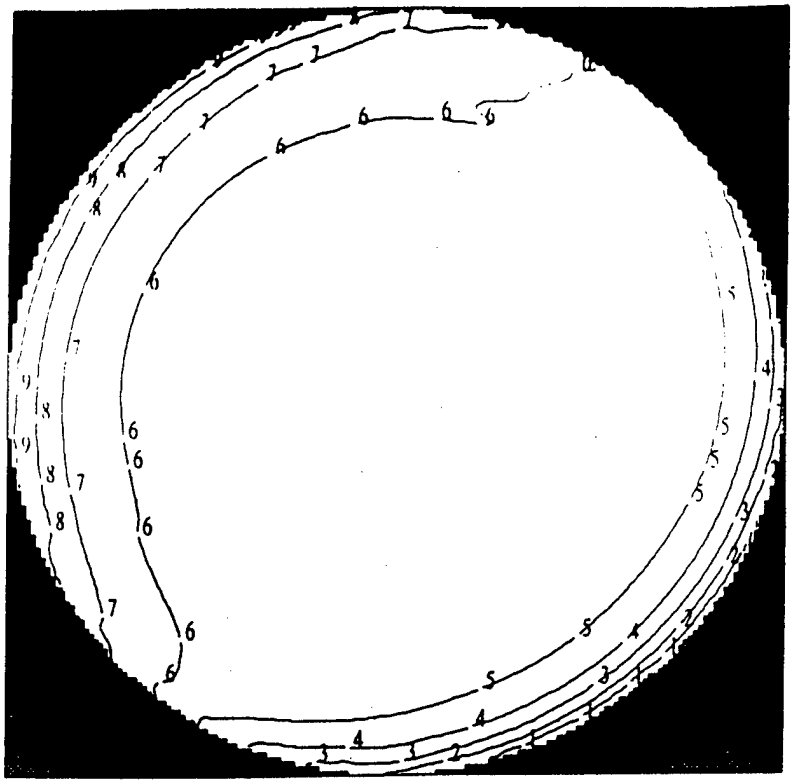

RigidBore625m: 1/2-day-averaged layer 4 temperatuer at day 6, depth= 9.7 m. min= 11.65. max= 13.68

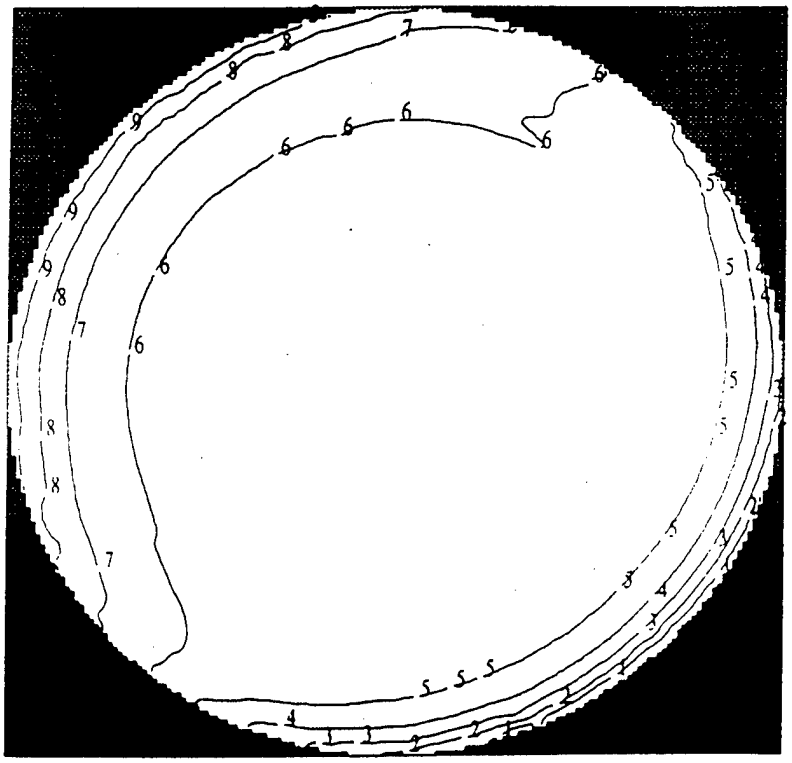

[illegible] 1/2 day-averaged layer 4 temperature at day 6, depth= 9.7 m. min= [illegible] max= 13.63

Figure 2: Comparison of time averaged results (over 1/2 day) from rigid-lid (top) and free-surface (bottom) models at Day 6.

DISTRIBUTION LIST

1. Scientific Officer
   Office of Naval Research
   800 N. Quincy Street
   Arlington, VA 22217-5000
   - Dr. Tom Curtin
   - Dr. Emanual Fiadeiro

2. Administrative Grants Officer
   Office of Naval Research Resident Representative
   101 Marietta Tower-Suite 2805
   101 Marietta Street
   Atlanta, GA 30303

3. Naval Research Laboratory
   Washinton, DC 20375
   - Director (Code 2627)
   - Dr. Rangarao Madala (Code 4320)

4. Defense Technical Information Center
   8725 John Kingman Road
   Suite 0944
   Fort Belvoir, VA 22060-6218

5. Oceanographer of the Navy
   U.S. Naval Observatory
   34th and Massachusetts
   Washington, DC 20392

6. Naval Research Laboratory
   Stennis Space Center, MS 39529
   - Technical Director
   - Dr. Charles Barron
   - Dr. John Harding
   - Dr. Harley Hurlburt
   - Dr. Paul Martin
   - Dr. Sylvia Murphy
   - Dr. Steve Piacsek
   - Dr. Ruth Prellor
   - Dr. Alex Warn-Varnas

7. Naval Oceanographic Office
   Stennis Space Center, MS 39529
   - Technical Director
   - Dr. Ted Bennett
   - Dr. Martha Head

8. Fleet Numerical Oceanographic Center
   Monterey, CA 93943-5000
   - Commanding Officer
   - Dr. Mike Clancy

9. Naval Meteorology & Oceanography Command
   Building 1020
   Stennis Space Center, MS 39529
   - Technical Director
   - Dr. George Heburn

10. Dr. Alan F. Blumberg
    HydroQual, Inc.
    1 Lethbridge Plaza
    Manwah, New Jersey 07430

11. Dr. Dong-Shan Ko
    170 Lake D'Este Drive
    Slidell, LA 70461

12. Texas A & M University
    Department of Oceanography
    College Station, TX 77843-3146
    - Dr. Leslie C. Bender
    - Dr. Doug Biggs
    - Dr. David A. Brooks
    - Dr. Norman L. Guinasso
    - Dr. Worth D. Nowlin, Jr.
    - Dr. Robert Reid

13. Dr. William Camp
Sandia National Laboratories
Albuquerque, NM 87185

14. Dr. Simon Chang
Naval Research Laboratory
Monterey, CA 93943-5006

15. University of Miami
RSMAS
4600 Rickenbacker Causeway
Miami, FL 33149
- Dr. Eric Chassignet
- Dr. Christopher N.K. Mooers

16. Naval Postgraduate School
Monterey, CA 93943
- Dr. Curtis A. Collins
- Dr. Peter Chu
- Dr. Robert Haney
- Dr. Le Ngoc Ly

17. Dr. Curt Covey
Lawrence Livermore Laboratory
University of California
P.O. Box 808, L-264
Livermore, CA 94550

18. Los Alamos National Laboratory
Los Alamos, NM 87545
- Dr. John Dukowicz
- Dr. Chick Keller
- Dr. Aaron Lai

19. Dr. Jay Fein
National Science Foundation
4201 Wilson Blvd., Room 725
Arlington, VA 22230

20. Dr. Michael Ghil
Atmospheric Sciences Department
UCLA
405 Hilgard Ave.
Los Angeles, CA 90024-1565

21. Dr. Dale Haidvogel
Rutgers University
Institute of Marine and Coastal Studies
P.O. Box 231
New Brunswick, NJ 08903-0231

22. Dr. Paola Rizzoli
Massachussets Institute of Technology
Cambridge, MA 02139

23. Florida State University
Tallahassee, FL 32306
- Dr. T.N. Krishnamurti
- Dr. James O'Brien
- Dr. Richard Pfeffer
- Dr. Tony Sturges
- Dr. George Weatherly

24. Dr. George Mellor
Princeton University
Geophysical Fluid Dynamics Laboratory
P.O. Box 308
Princeton, NJ 08540

25. Dr. Alberto Mestas-Nunez
NOAA/AOML
4301 Rickenbacker Causeway
Miami, FL 33149

26. Scripps Institute of Oceanography
San Diego, CA 92093
- Dr. Peter Niiler
- Dr. Richard Somerville

27. State University of New York
Stony Brook, NY 11794
- Dr. Dong-Ping Wang
- Dr. Robert Wilson

28. Oregon State University
College of Oceanography
Corvallis, OR 97331-5503
- Dr. Tim F. Pugh
- Dr. Jim Richman
- Dr. John Allen

29. Dr. William P. O'Connor
NOAA/NOS
1315 East-West Highway, Rm 7711
Silver Springs, MD 20910-3282

30. Dr. David J. Schwab
NOAA Great Lakes Environmental
Research Laboratory
2205 Commonwealth Blvd.
Ann Arbor, MI 48105-1593

31. Dr. Leonard J. Walstad
Center for Environmental and
Estuarine Studies
University of Maryland
P.O. Box 775
Cambridge, MD 21613-0775

32. Dr. Joannes J. Westerink
University of Notre Dame
Notre Dame, IN 46117

33. Dr. David Szabo
Mobil Research and Development
Corporation
13777 Midwam Road
Farmers Branch, TX 75234

34. Marathon Oil Company
P.O. Box 3128
Houston, TX 77253
- Dr. Kenneth J. Schaudt

35. Dr. Ken Nibbelink
Amoco Production
P.O. Box 3092
Houston, TX 77253-3092

36. Dr. Cort Cooper
Chevron Petroleum Technology
1300 Beach Blvd.
La Habra, CA 90631

37. Dr. Lance Bode
James Cook University
Townsville, QLD 4811
AUSTRALIA

38. Dr. Ian Webster
CSIRO
GPO Box 821
Canberra, ACT 2601
AUSTRALIA

39. CSIRO
Box 1538
Hobart, TAS 7001
AUSTRALIA
- Dr. George Cresswell
- Dr. Scott Condie
- Dr. Angus McEwan

40. Dr. Cliff Hearn
Australian Defense Force Academy
Canberra, ACT 2600
AUSTRALIA

41. Dr. John L. McGregor
Climate Modeling Program
PMB1 Aspendale, Vic 3195
AUSTRALIA

42. CDR Martin Rutherford
Maritime Headquarters-Wylde Street
Potts Point NSW 2011
AUSTRALIA

43. Dr. Brian Sanderson
University of New South Wales
Sydney, NSW 2052
AUSTRALIA

44. Dr. Jinyu Sheng
Memorial University
St. John's, Newfoundland
CANADA A1B 3X7

45. Dr. Dan Wright
Bedford Institute of Oceanography
Dartmouth, N.S.
CANADA B2Y 4A2

46. Dr. Emil Stanev
University of Sofia
5, James Bourchier Street
1126 Sofia
BULGARIA

47. Dalhousie University
Halifax, NS
CANADA B3H 4J1
- Dr. Richard Greatbatch
- Dr. Keith Thompson

48. Institute of Ocean Sciences
P.O. Box 6000
Sidney, B.C.
CANADA V8L 4B2
- Dr. Greg Holloway
- Dr. Josef Cherniowski

49. McGill University
805 Sherbrooke Street West
Montreal, Quebec
CANADA H3A 2K6
- Dr. Jacques Derome
- Dr. Charles Lin

50. Dr. Chris Garrett
University of Victoria
P.O. Box 1700
Victoria, B.C.
CANADA V8W 2Y2

51. Dr. Malcolm Bowman
University of Auckland
PO Box 92019
Auckland, NEW ZEALAND

52. Dr. Ross Vennell
University of Otago
304 Castle Street
Dunedin, NEW ZEALAND

53. Dr. Richard Wood
The Meteorological Office
London Road
Bracknell, Berkshire
RG12 2SY UNITED KINGDOM

54. Dr. Rob C. Murdoch
NIWA
P.O. Box 14-901 Kilbirnie
Wellington, NEW ZEALAND

55. Dr. Alan Davies
Proudman Oceanographic Laboratory
Bidston Observatory
Birkenhead, Merseyside
L43 7RA UNITED KINGDOM

56. Dr. Lindsay H Hall
NZ Defence Force
Private Bag 32901
Auckland, NEW ZEALAND

REPORT DOCUMENTATION PAGE

Form Approved
OMB No. 0704-0188

1. Agency Use Only *(Leave blank).*	2. Report Date.	3. Report Type and Dates Covered.
	15 April 1998	TECHNICAL REPORT

4. Title and Subtitle.

A SEMI-IMPLICIT FREE SURFACE FORMULATION FOR THE SEMI-COLLOCATED GRID DIECAST OCEAN MODEL

5. Funding Numbers.

Program Element No.

Project No.

Task No.

Accession No.

6. Author(s).

David E. Dietrich and Avichal Mehra

7. Performing Organization Name(s) and Address(es).

Mississippi State University
Center for Air Sea Technology
Stennis Space Center, MS 39529-6000

8. Performing Organization Report Number.

CAST Technical Report 3-98

9. Sponsoring/Monitoring Agency Name(s) and Address(es).

Office of Naval Research
800 North Quincy Street
Arlington, VA 22217-5000

10. Sponsoring/Monitoring Agency Report Number.

Report 3-98

11. Supplementary Notes.

Research performed under Office of Naval Research Grants No. N00014-97-1-0525 and N00014-97-1-0099.

12a. Distribution/Availability Statement.

Approved for public release; distribution is unlimited

12b. Distribution Code.

13. Abstract *(Maximum 200 words).*

Under funding from the Office of Naval Research (ONR), the Mississippi State University Center for Air Sea Technology (CAST) presents a semi-implicit free-surface formulation for the DieCAST Ocean model that retains the accurate, low dissipation numerics of its latest and best semi-collocated rigid-lid version. The approach involves integrating the time-implicit (trapezoidal) shallow water equations on a staggered Arakawa "c" grid, with vertically averaged baroclinic forcing terms determined on a non-staggered Arakawa "a" grid, including a fourth-order-accurate baroclinc pressure gradient. The shallow water equation numerics are virtually equivalent to standard sigma coordinate approaches for the model barotropic mode. In application to transient wind forced lake Kelvin waves, the new free-surface version gives virtually identical results to the corresponding strongly validated rigid-lid DieCAST version (reflecting the fact that the rigid-lid barotropic mode numerics are also a sigma-like approach,) and requires less than 50 percent more computing. Thus, the numerics used by both rigid-lid and free-surface DieCAST versions combines the best of z-level and sigma coordinate numerics, as well as, the best of "a" and "c" grid numerics.

14. Subject Terms.	15. Number of Pages.
(U) DIECAST (U) OCEAN (U) MODEL (U) FREE SURFACE (U) RIGID-LID (U) GRID (U) SEMI-IMPLICIT	22
	16. Price Code.

17. Security Classification of Report.	18. Security Classification of This Page.	19. Security Classification of Abstract.	20. Limitation of Abstract.
UNCLASSIFIED	UNCLASSIFIED	UNCLASSIFIED	